C.2

NACA

RESEARCH MEMORANDUM

for the

Bureau of Aeronautics, Department of the Navy

ROCKET-MODEL INVESTIGATION OF THE LONGITUDINAL STABILITY

AND DRAG CHARACTERISTICS OF A 1/10-SCALE MODEL OF THE

CONVAIR XF2Y-1 AIRPLANE HAVING OPEN DUCTS AND THE

ELEVONS DEFLECTED UPWARD 3.5°

TED NO. NACA DE 375

By Clement J. Welsh, William M. Bland, Jr.,
and Richard E. Walters

Langley Aeronautical Laboratory
Langley Field, Va.

NATIONAL ADVISORY COMMITTEE
FOR AERONAUTICS
WASHINGTON

NATIONAL ADVISORY COMMITTEE FOR AERONAUTICS

RESEARCH MEMORANDUM

for the

Bureau of Aeronautics, Department of the Navy

ROCKET-MODEL INVESTIGATION OF THE LONGITUDINAL STABILITY

AND DRAG CHARACTERISTICS OF A 1/10-SCALE MODEL OF THE

CONVAIR XF2Y-1 AIRPLANE HAVING OPEN DUCTS AND THE

ELEVONS DEFLECTED UPWARD 3.5°

TED NO. NACA DE 375

By Clement J. Welsh, William M. Bland, Jr.,
and Richard E. Walters

SUMMARY

A 1/10-scale rocket-propelled model of the Convair XF2Y-1 airplane having open ducts and the elevons deflected upward 3.5° has been flight tested by the Langley Pilotless Aircraft Research Division through a Mach number range of about 0.7 to 1.5.

Test results indicated the following conclusions: There was a drag rise of approximately 0.020, with a peak supersonic drag coefficient of about 0.036 at $M = 1.1$; a helium-gun equivalent-area model had a similar drag rise. The lift-curve slopes for the total configuration were approximately 0.058, 0.046, and 0.042 for corresponding Mach numbers of 0.91, 1.22, and 1.49. There was a slight rearward movement of the aerodynamic center at supersonic speeds from approximately 41 percent mean aerodynamic chord at $M = 0.91$.

INTRODUCTION

The second model of a series of 1/10-scale rocket-propelled models of the Convair XF2Y-1 airplane being tested at the request of the Bureau of Aeronautics, Department of the Navy, has been flown. The Convair XF2Y-1, which is a twin-turbojet-engined tailless airplane with modified delta

wings and vertical surface, is designed to be a water-based supersonic fighter airplane.

The primary purpose of this flight, which was conducted at the Langley Pilotless Aircraft Research Station at Wallops Island, Va., was to determine the aerodynamic characteristics of this model with air flow through the open ducts which will house the turbojet engines on the full-scale airplane.

The longitudinal stability and drag characteristics obtained from the flight test of the model are presented in this paper for a Mach number range of 0.7 to 1.5 which corresponds to a Reynolds number range of 8.4×10^6 to 22×10^6. In order to facilitate the publishing of the data no analysis is presented.

SYMBOLS

S	total included wing area, sq ft
$\bar{c}$	wing mean aerodynamic chord, ft
A	cross-sectional area of equivalent body, sq in.
r_{equiv}	radius of equivalent body of revolution, in.
l	body length, in.
X	distance from nose, in.
I_Y	moment of inertia about pitching axis, slug-sq ft
M	free-stream Mach number
R	Reynolds number
q_0	free-stream dynamic pressure, lb/sq ft
α	angle of attack, deg
p_a	atmospheric static pressure, lb/sq ft
p	local static pressure, lb/sq ft
P	pressure coefficient, $\dfrac{p - p_a}{q_0}$

g   acceleration due to gravity, 32.2 ft/sec^2

x   distance between nose and center-of-gravity normal accelerometers

a_N normal accelerometer reading, g units

C_N normal-force coefficient, $\dfrac{\text{Normal force}}{q_0 S}$

C_C chord-force coefficient, $\dfrac{\text{Chord force}}{q_0 S}$

C_L lift coefficient

C_D drag coefficient

C_m pitching-moment coefficient relative to 18.65 percent $\bar{c}$

C_{m_α} moment-curve slope

C_{L_α} lift-curve slope

$C_{m_q} + C_{m_{\dot{\alpha}}}$ damping-in-pitch coefficient, $\dfrac{dC_m}{d\left(\frac{q\bar{c}}{2V}\right)} + \dfrac{dC_m}{d\left(\frac{\dot{\alpha}\bar{c}}{2V}\right)}$

H_D duct total pressure, lb/sq ft

H_0 free-stream total pressure, lb/sq ft

m_D duct mass flow

m_0 mass flow through a free-stream tube of the same area as the duct inlet

V   free-stream velocity, ft/sec

V_e duct-exit velocity, ft/sec

M_e duct-exit Mach number

p_e duct-exit static pressure, lb/sq ft

A_e duct-exit area, sq in.

A_i duct-inlet area, sq in.

$\dot{\alpha}$ $\dfrac{d\alpha}{dt}$, radians/sec

q $\dfrac{d\theta}{dt}$, pitching velocity, radians/sec

$\ddot{\theta}$ pitching acceleration, radians/sec^2

γ ratio of specific heats

θ angle of pitch, radians

Subscripts:

t   trim conditions

B   beach (rear portion of fuselage behind the exits)

cg   center of gravity

int   internal

MODELS AND TESTS

A sketch of the Convair XF2Y-1 rocket model is shown in figure 1 and photographs of the configuration are presented as figure 2. Two helium-gun equivalent-area models have also been tested by the technique as described in reference 1. One of these models was of the Convair XF2Y-1 corresponding to a rocket-model duct mass-flow ratio of about 0.73. The second helium-gun model was of the Convair F2Y-1 airplane corresponding to a mass-flow ratio of 1.0. The longitudinal area distributions and the model profiles of the tested configurations are shown in figure 3.

The rocket-model fuselage was constructed of plastic-fiberglass laminate. The wing and tail construction was of laminated wood with aluminum-alloy inlays.

As the first rocket model of the XF2Y-1 tested was laterally unstable (ref. 2), an analysis of its dynamic lateral stability charac-teristics was made. The analysis indicated that the instability of the model was the result of its negative trim angle of attack combined with the condition that the longitudinal principal axis of the model was below the body axis.

In order to alleviate these adverse stability characteristics on the present model, the elevons were deflected upward 3.5° for a higher model trim angle and ballast was added to raise the principal axis and to move the center of gravity forward.

The ducts, which on the full-scale airplane house the turbojet engines, were left open in order that the effects of air flow through the ducts would be included in the present test. A sketch of the rocket-model duct cross-sectional area is shown in figure 4; also shown is a sketch of the duct inlet which is on the full-scale airplane. As the rocket-model ducts did not contain boundary-layer splitter plates, the cross-sectional inlet area of the rocket model differed from that of the full-scale airplane as indicated in figure 4. The duct pressures were measured at duct longitudinal positions as listed in figure 4, with four static-pressure orifices manifolded together on the duct wall and the total pressure orifice at the center of the duct.

In order to produce disturbances of the model in pitch about its lateral axis during flight, in such a manner that longitudinal stability data could be obtained, two pulse rockets were installed in the rear portion of the fuselage.

The model was equipped with a ten-channel telemeter to transmit data during its flight. Measurements made included longitudinal acceleration, transverse acceleration, normal acceleration near the center of gravity and in the nose of the model, angle of attack, free-stream total pressure, duct static and total pressure, base pressure, and pressure measurements over the beach of the model. The base and beach pressure measurements refer to the duct-exit annular areas and the rear portion of the configuration as indicated in figure 2(c) which also shows the various pressure-orifice locations.

The model was launched at a 60° elevation angle and boosted to its maximum Mach number by a 6-inch-diameter solid-fuel ABL deacon rocket motor. The model did not contain a sustainer rocket motor.

The CW Doppler radar velocimeter and the SCR 584 radar were used to obtain the velocity and the flight path of the model. Atmospheric conditions at the time of the flight were determined from radiosonde data. The Reynolds number of the test configurations varied with Mach number as shown in figure 5.

<center>ACCURACY</center>

Experience has indicated that the errors in a measured telemeter quantity are within ± 1 percent of the range of the instrument; hence,

errors in telemeter quantities translated into coefficient form are
within the values listed in the following table:

M	C_N	C_C	P
1.5	±0.002	±0.001	±0.0013
.9	±.006	±.002	±.004

Errors in Mach number and $\Delta\alpha$ are believed to be within ±0.015
and ±0.10°, respectively, throughout the test range.

RESULTS AND DISCUSSION

Lift and Stability

During the flight there were three disturbances of the model about
its pitching axis of about 2° or 3° in angle of attack from trim con-
ditions. The first disturbance occurred at the time of the separation
of the model from the booster and the other two were from the pulse
rockets. As there were no appreciable transverse accelerations during
the flight, the short-period oscillations in pitch resulting from these
disturbances have been analyzed by the methods of reference 3. In
addition, the data from the two normal accelerometers were used to
obtain total pitching-moment data as follows:

The pitching acceleration $\ddot{\theta}$ is given by

$$\ddot{\theta} = \frac{g}{x}\left[\left(a_N\right)_{nose} - \left(a_N\right)_{cg}\right]$$

which is proportional to the total pitching-moment coefficient

$$C_m = \frac{I_y}{q_0 S\bar{c}}\ddot{\theta}$$

Typical variations of C_L and C_m with angle of attack are shown
in figure 6. Test points are shown to give an indication of the accuracy
of the data. A nearly linear variation exists for both C_L and C_m
with α for the test range of α.

Values of C_{L_α}, C_{m_α}, dC_m/dC_L, and $C_{m_q} + C_{m_{\dot\alpha}}$ are shown in figure 7 plotted against Mach number.

Values of C_{L_α} for the total configuration were approximately 0.058, 0.046, and 0.042 for corresponding Mach numbers of 0.91, 1.22, and 1.49. Relative to the C_{L_α} of 0.03 at $M = 1.53$, as determined for the first XF2Y-1 rocket model (ref. 2), it is now believed that the effect of the lateral motion of the model on the measured C_{L_α} value was greater than previously assumed. The C_{m_α} values as calculated from the period of the free oscillation of the model are in agreement with the C_{m_α} values as determined from the normal accelerometer measurements.

The values of dC_m/dC_L calculated by three methods have been plotted (fig. 7). The methods used in obtaining dC_m/dC_L were: (a) directly from its proportional relationship to $\dfrac{d(a_N/g)_{nose}}{d(a_N/g)_{cg}} - 1$ (assuming that $dC_m/dC_n = dC_m/dC_L$ for the existing small range of α); (b) from the quotient of C_{m_α} and C_{L_α} where C_{m_α} was determined from the period of the free oscillation; and (c) from the quotient of C_{m_α} and C_{L_α} where C_{m_α} was obtained from the normal accelerometers. The values of dC_m/dC_L obtained by the three methods are in agreement and, combined with the configuration center-of-gravity position at 18.65 percent $\bar{c}$, indicate aerodynamic-center locations in percent $\bar{c}$ of about 41, 44, and 44 for corresponding Mach numbers of 0.91, 1.22, and 1.49.

The small magnitude of the combined damping-in-pitch derivatives $C_{m_q} + C_{m_{\dot\alpha}}$ is consistent with other configurations not having horizontal tails.

Variations of lift coefficient and angle of attack for trim conditions with Mach number are shown in figure 8. The trim curves as shown were determined from the record; the dashed sections of the curves indicate a mean line through an oscillation. The individual points as plotted were obtained from figure 6.

The variation of the pressure coefficient over the beach of the model with Mach number is shown in figure 9. Also shown are a sketch and table defining the beach surface. The origin of the sketch for any given station is on a line intersecting the center of the duct-exit area and parallel to the longitudinal axis of the model.

The beach pitching-moment coefficient C_{m_B} has been plotted against Mach number in figure 10 to give an indication of the contribution of the

beach to the total pitching moment of the configuration (with air flow through the ducts). The C_{m_B} values have been calculated by the method used and described in detail in reference 2 from pressure measurements made over the beach.

Drag

The variation of the total drag coefficient of the Convair XF2Y-1 rocket model with Mach number is shown in figure 11(a); also shown are the drag curves of the two helium-gun models of the XF2Y-1 rocket model and F2Y-1 airplane. The measured component drag coefficients of the rocket-model plotted against Mach number are shown in figure 11(b).

The drag coefficient for the rocket model having open ducts is approximately 0.015 at subsonic speeds increasing to about 0.036 at $M = 1.1$ and then decreasing slightly with further increasing Mach number. The transonic drag rise for the XF2Y-1 helium-gun model of about 0.020 is in agreement with that of the rocket model.

The base drag for this configuration, which is defined as that drag attributed to the annular areas of the duct exits as indicated in figure 2(c), has been calculated from pressure measurements made on the annulus of the port exit.

The beach drag refers to the drag of the rear portion of the configuration immediately behind the duct exits, as indicated in figure 2(c). The drag coefficients have been calculated by the method described in detail in reference 2 from pressure measurements.

The internal drag for this configuration is defined as the drag resulting from the air flow through the two open ducts. The coefficients were calculated by the use of the expression

$$C_{D_{int}} = \left[m_D(V - V_e) + A_e(p_a - p_e) \right] \frac{1}{q_0 S}$$

The internal drag represents about 1 to 6 percent of the total drag of the configuration for the test range of Mach number.

Duct Flow

The mass flow and pressure recovery ratios of the ducts as a function of Mach number are shown in figure 12. The mass-flow ratio was determined from the expression

$$\frac{m_D}{m_0} = \frac{p_e M_e \left(1 + \frac{\gamma - 1}{2} M_e^2\right)^{1/2}}{p_a M \left(1 + \frac{\gamma - 1}{2} M^2\right)^{1/2}} \frac{A_e}{A_i}$$

which gives a nearly constant value of 0.7 over the Mach number range of the test. Choking conditions at the duct exits at supersonic speeds were assumed in the mass-flow calculations.

The pressure recovery ratio of the ducts refers to the ratio of the duct total pressure to that of the free stream.
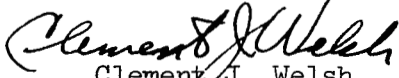
CONCLUSIONS

A 1/10-scale rocket-propelled model of the Convair XF2Y-1 airplane having open ducts and the elevons deflected upward $3.5°$ has been flight tested to determine its longitudinal stability and drag characteristics over a Mach number range from about 0.7 to 1.5. The data indicate the following conclusions:

1. There is a transonic drag rise of approximately 0.020, with a peak supersonic drag coefficient of about 0.036 at $M = 1.1$; a helium-gun equivalent-area model had a similar drag rise.

2. The lift-curve slopes for the total configuration were approximately 0.058, 0.046, and 0.042 for corresponding Mach numbers of 0.91, 1.22, and 1.49.

3. There was a slight rearward movement of the aerodynamic center at supersonic speeds from approximately 41 percent of the mean aerodynamic chord at $M = 0.91$.
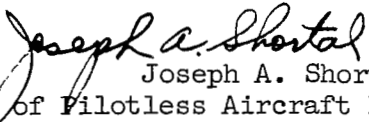
Langley Aeronautical Laboratory,
        National Advisory Committee for Aeronautics,
            Langley Field, Va., December 22, 1953.

Clement J. Welsh
Aeronautical Research Scientist

William M. Bland, Jr.
Aeronautical Research Scientist

Richard E. Walters
Aeronautical Research Scientist

Approved:
                Joseph A. Shortal
        Chief of Pilotless Aircraft Research Division

mhg

REFERENCES

1. Hall, James Rudyard: Comparison of Free-Flight Measurements of the
   Zero-Lift Drag Rise of Six Airplane Configurations and Their
   Equivalent Bodies of Revolution at Transonic Speeds. NACA
   RM L53J21a, 1953.

2. Bland, William M., Jr., and Nelson, Robert L.: Results of a Power-On
   Flight of a 1/10-Scale Rocket-Propelled Model of the Convair XF2Y-1
   Airplane at a Mach Number of 1.53 — TED No. NACA DE 365. NACA
   RM SL53I30a, Bur. Aero., 1953.

3. Gillis, Clarence L., Peck, Robert F., and Vitale, A. James: Pre-
   liminary Results From a Free-Flight Investigation at Transonic and
   Supersonic Speeds of the Longitudinal Stability and Control Charac-
   teristics of an Airplane Configuration With a Thin Straight Wing of
   Aspect Ratio 3. NACA RM L9K25a, 1950.

Weight .... 94.6 lb
Moment of inertia about
  pitching axis .... 4.37 slug ft^2
Inclination of principal axis
  below body axis .... 0.5°
Center of gravity .... 18.65 percent M.A.C.

Wing
  Total area .... 5.63 ft^2
  Aspect ratio 2.03
  Elevon deflection .... 3.5° upward
  Airfoil section
    at centerline .... NACA 0002.89-65 (modified)
    from 86 percent of
    half-span to tip .... NACA 0004-65 (modified)

Tail
  Exposed area .... 0.80 ft^2
  Airfoil section
    at root .... NACA 0003-65 (modified)
    at tip .... NACA 0004-65 (modified)

Angle-of-attack indicator

20.20

Elevon

M.A.C.

60°

17.49

29.86

25.69

18.69

2.65

56°

15.20

4.20

Dihedral angle
1° 22' 27"

12.50

40.40

62.70

Station 0
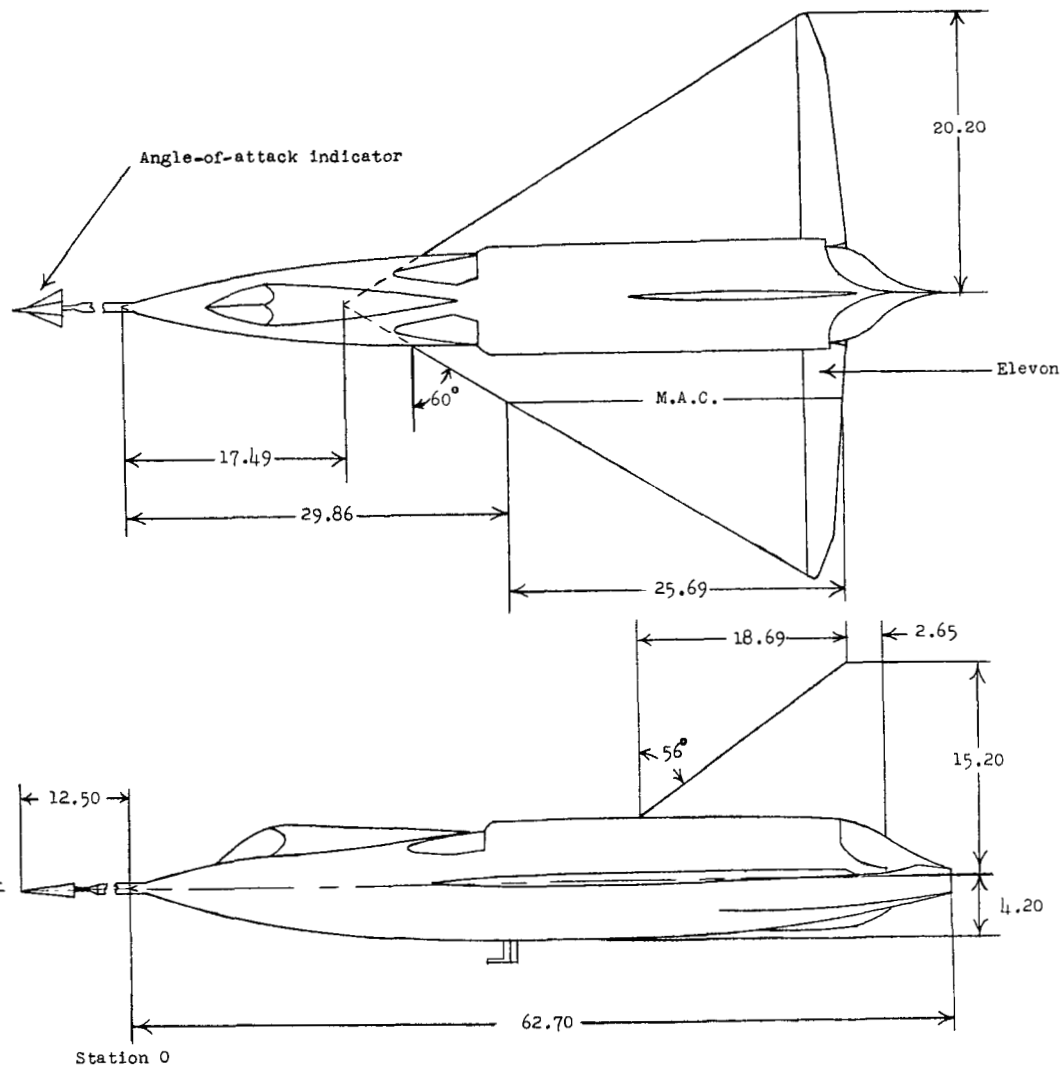
Figure 1.- General arrangement of the rocket model. (All linear
dimensions in inches.)
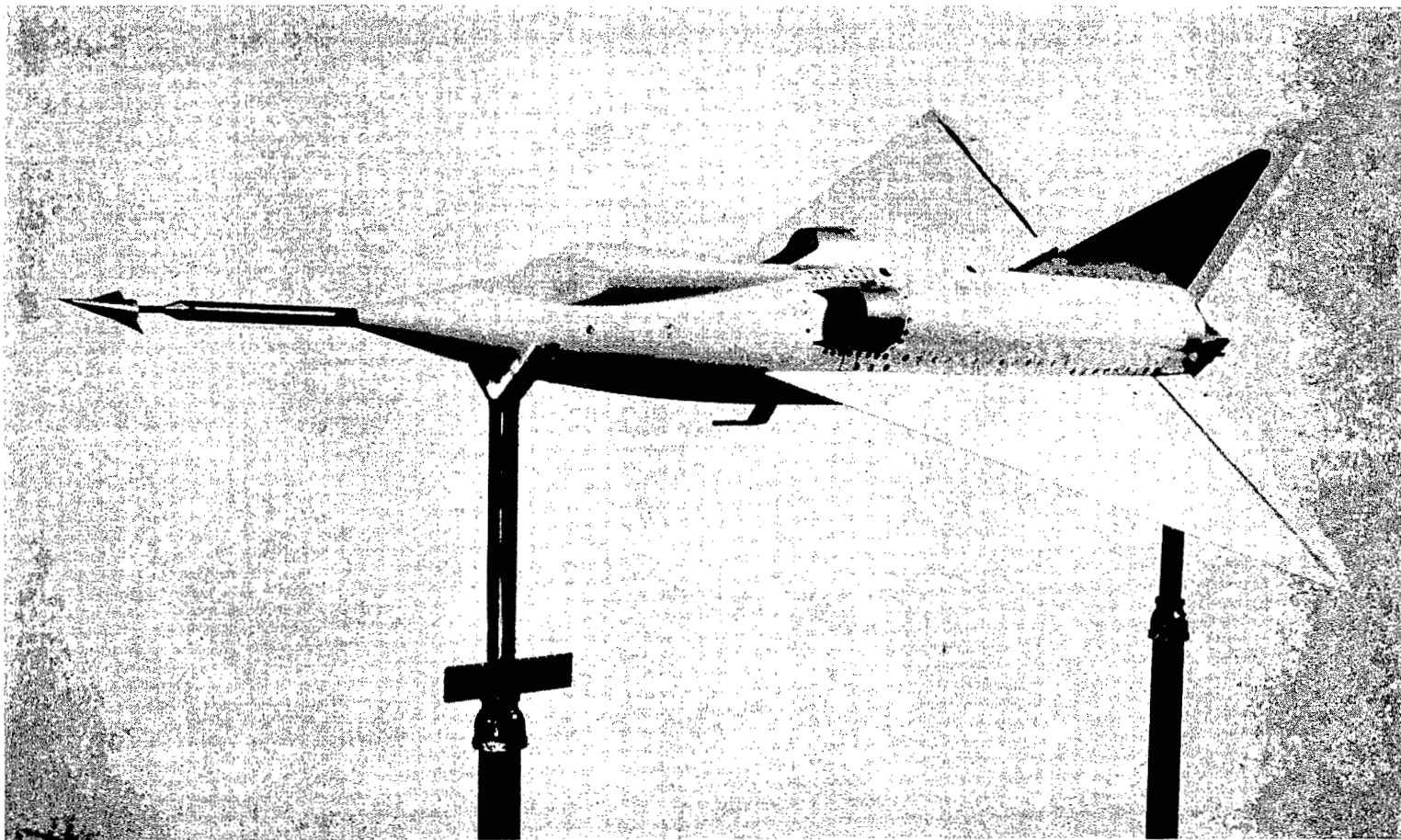
L-78832.1

(a) One-quarter view.

Figure 2.- Photographs of model.
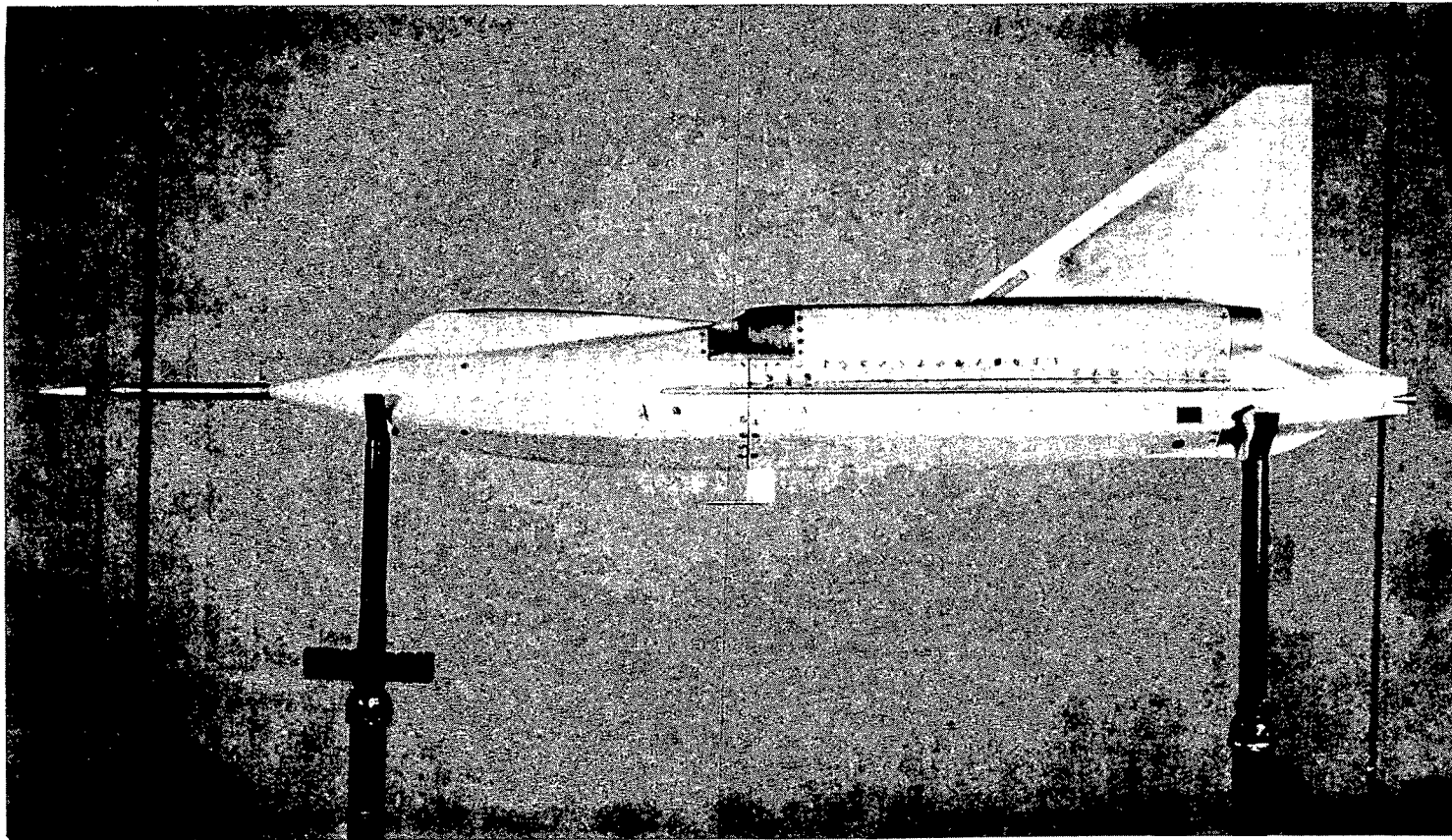
(b) Side view.   L-78835.2

Figure 2.- Continued.
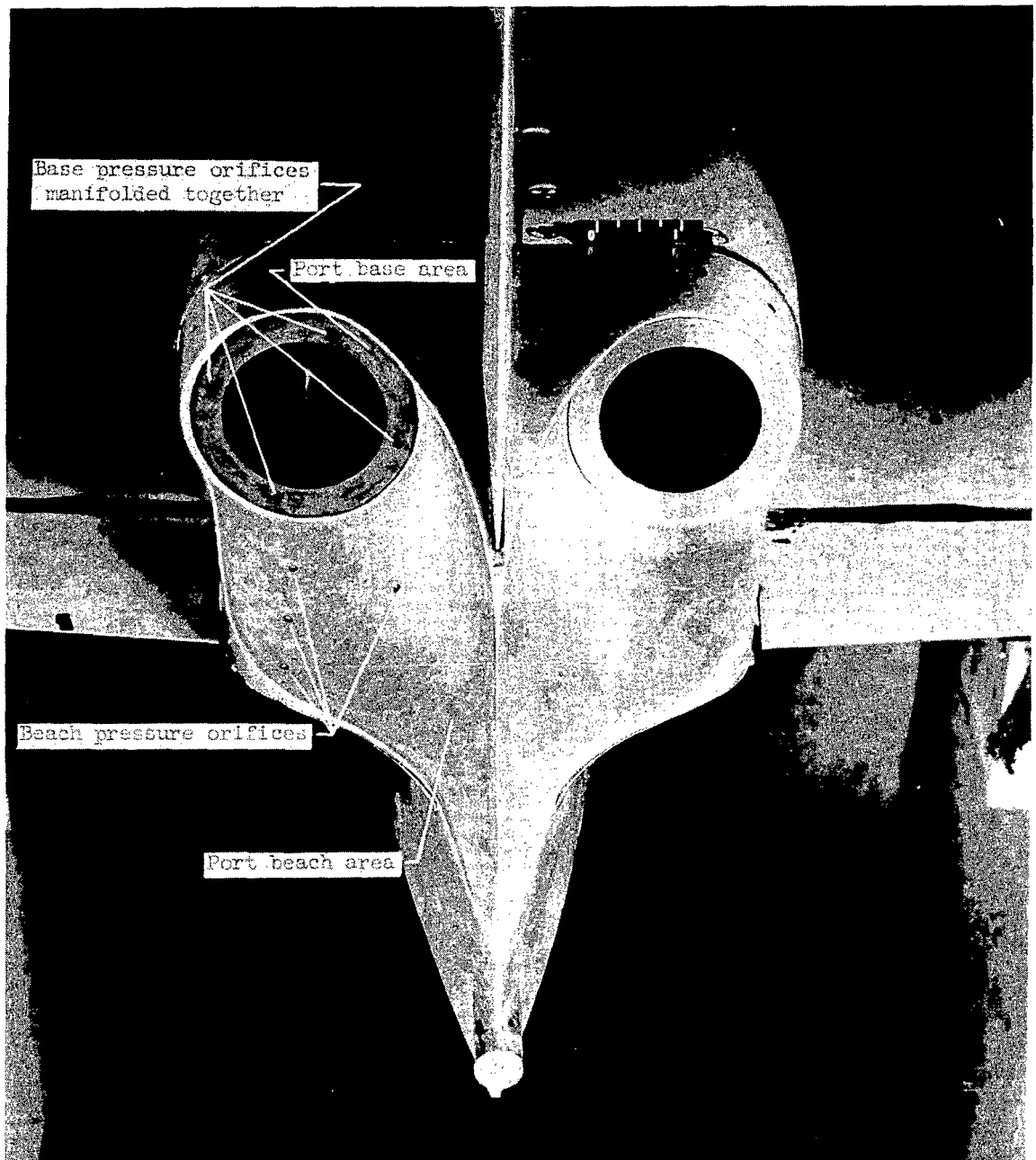
(c) Rear view.   L-78839.1

Figure 2.- Concluded.

Rocket model

r_{equiv}/l
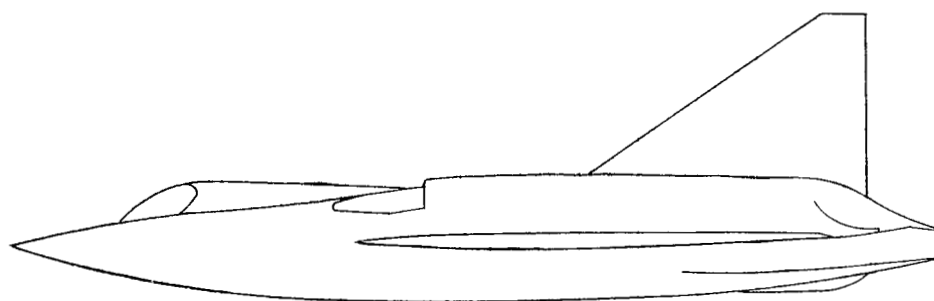
X/l
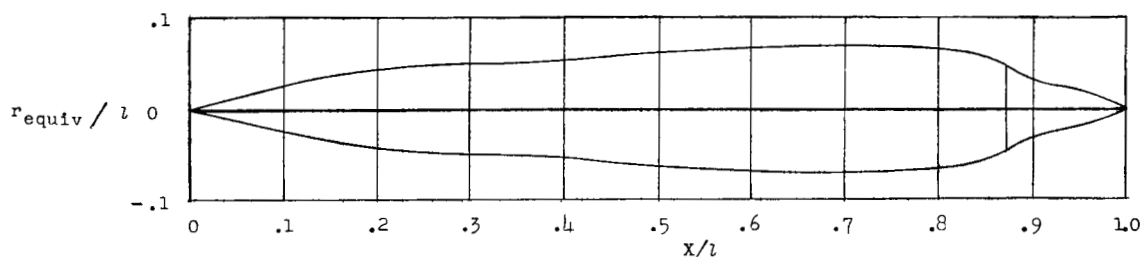
Profile of the equivalent body, corresponding
to a duct mass-flow ratio of 0.73.

A/l^2

Total
(mass-flow ratio = 0)

Total
(mass-flow ratio = 0.73)

Wing (rocket model)

Tail (rocket model)

X/l
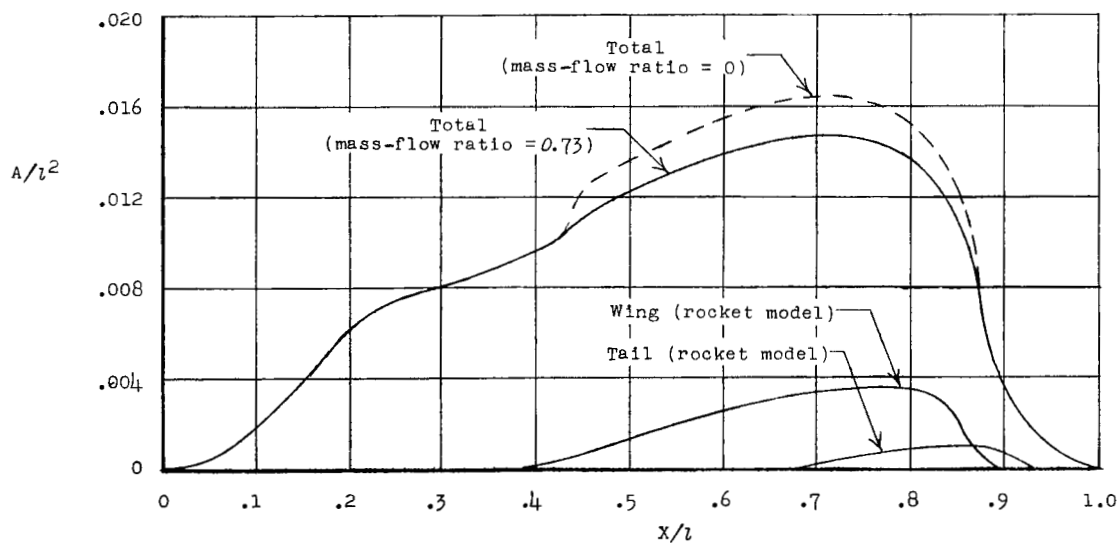
Longitudinal area distribution

(a) Rocket and helium-gun models of the Convair XF2Y-1.

Figure 3.- Physical characteristics of the test configurations.

Profile of the equivalent-area model.

Longitudinal area distribution corresponding to
a duct mass-flow ratio of 1.0
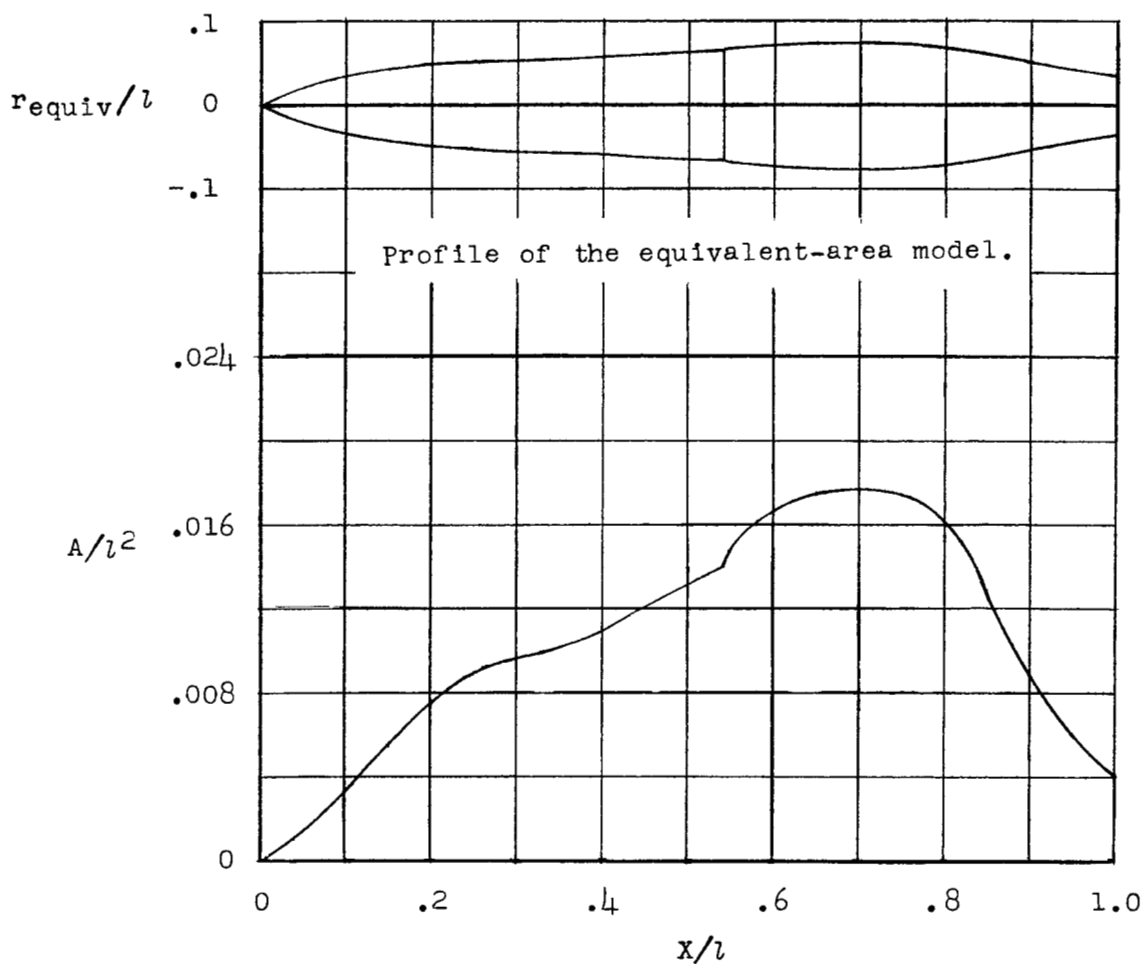
(b) Helium-gun model of the F2Y-1.

Figure 3.- Concluded.
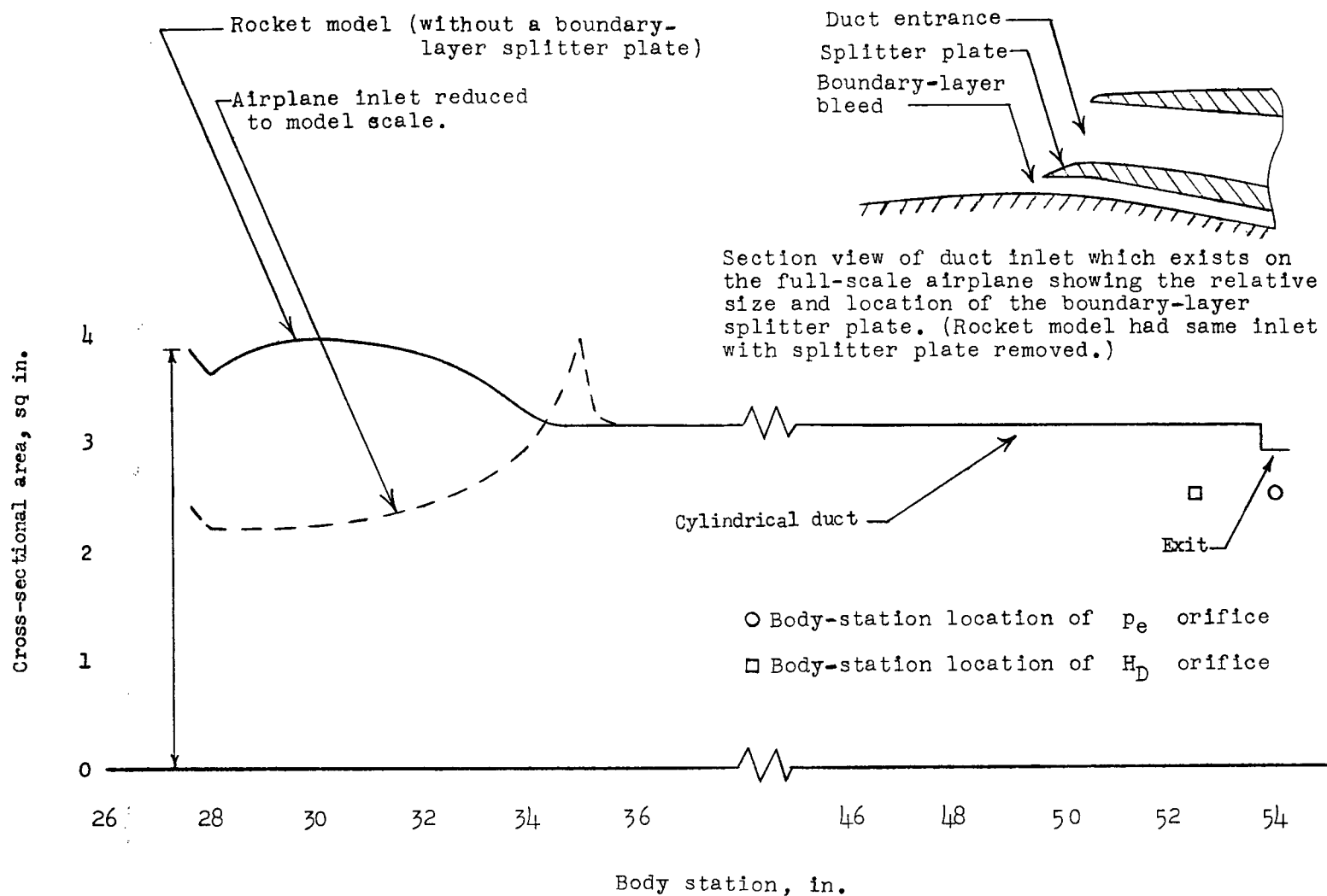
Figure 4.- Variation of the cross-sectional area of one duct with body
station for the Convair XF2Y-1 rocket model.
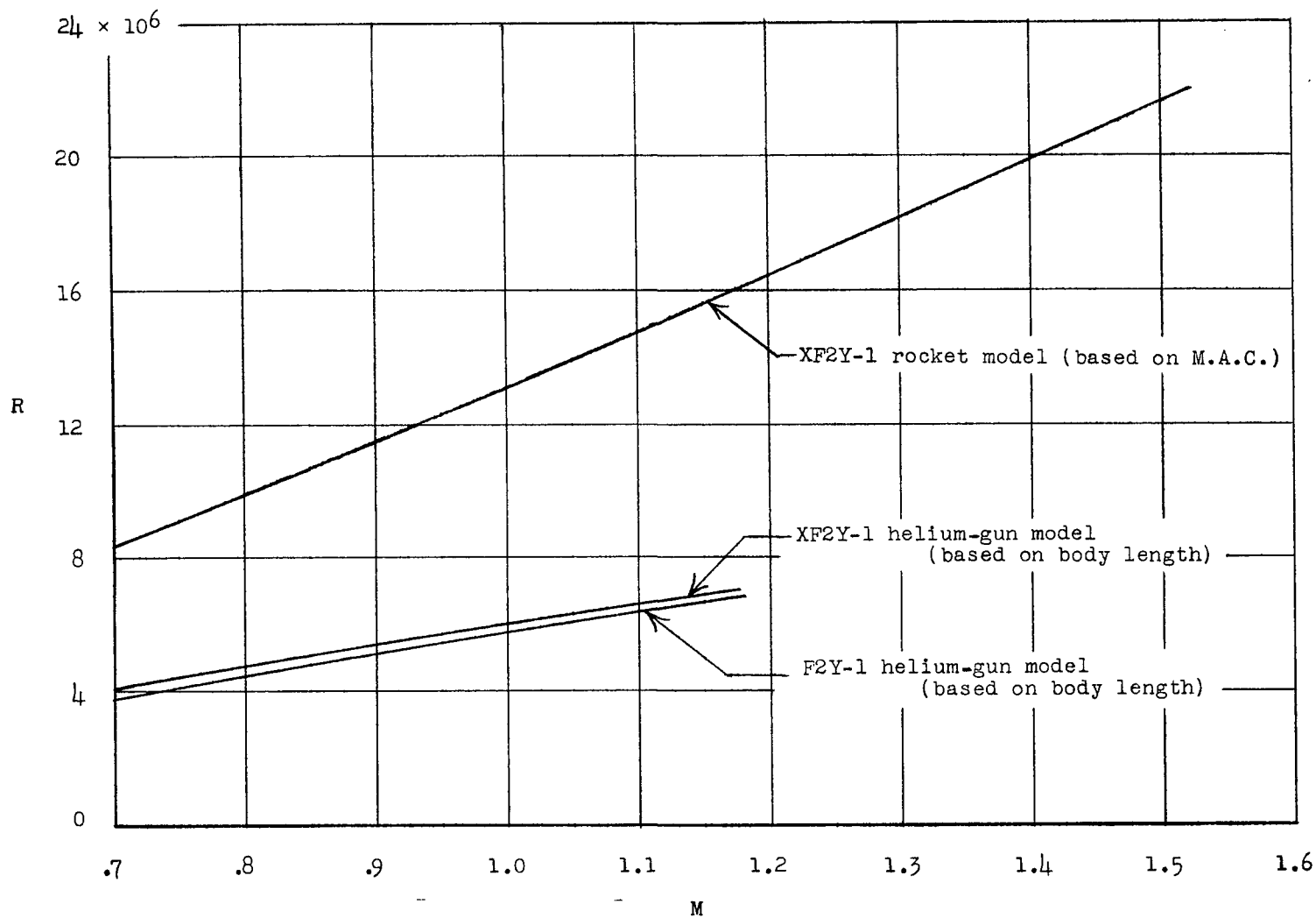
Figure 5.- Variation of Reynolds number with Mach number for the test
configurations.
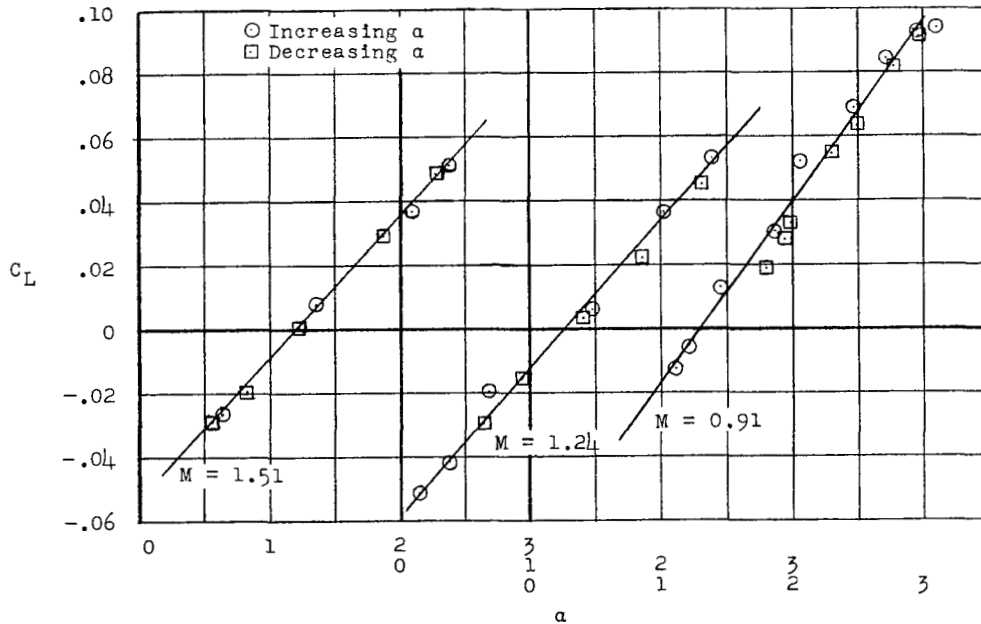
(a) Lift coefficient.
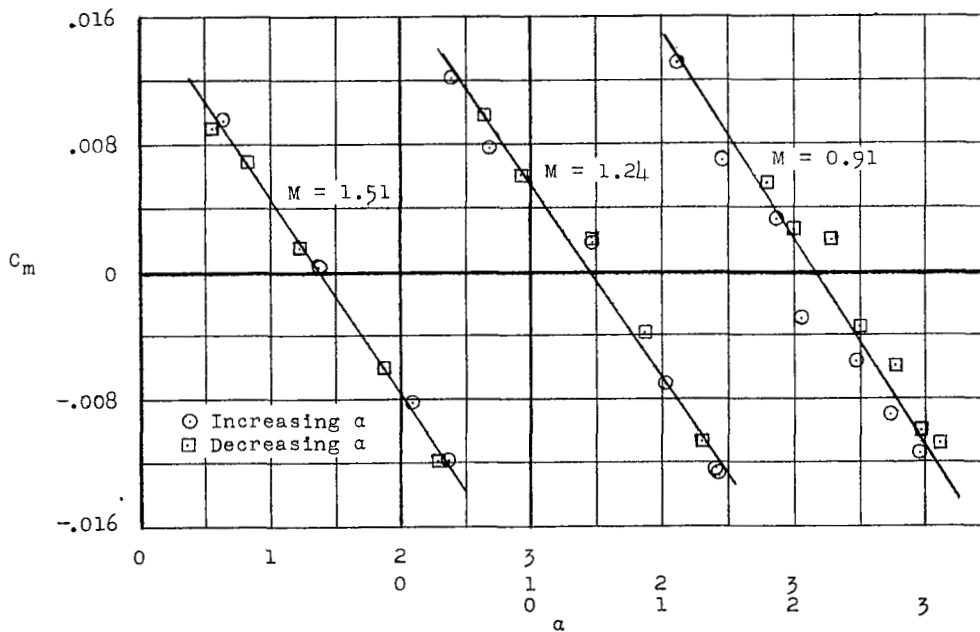
(b) Moment coefficient.

Figure 6.- Typical variations of lift coefficient and moment coefficient with angle of attack. (Model center of gravity at 18.65 percent mean aerodynamic chord.)
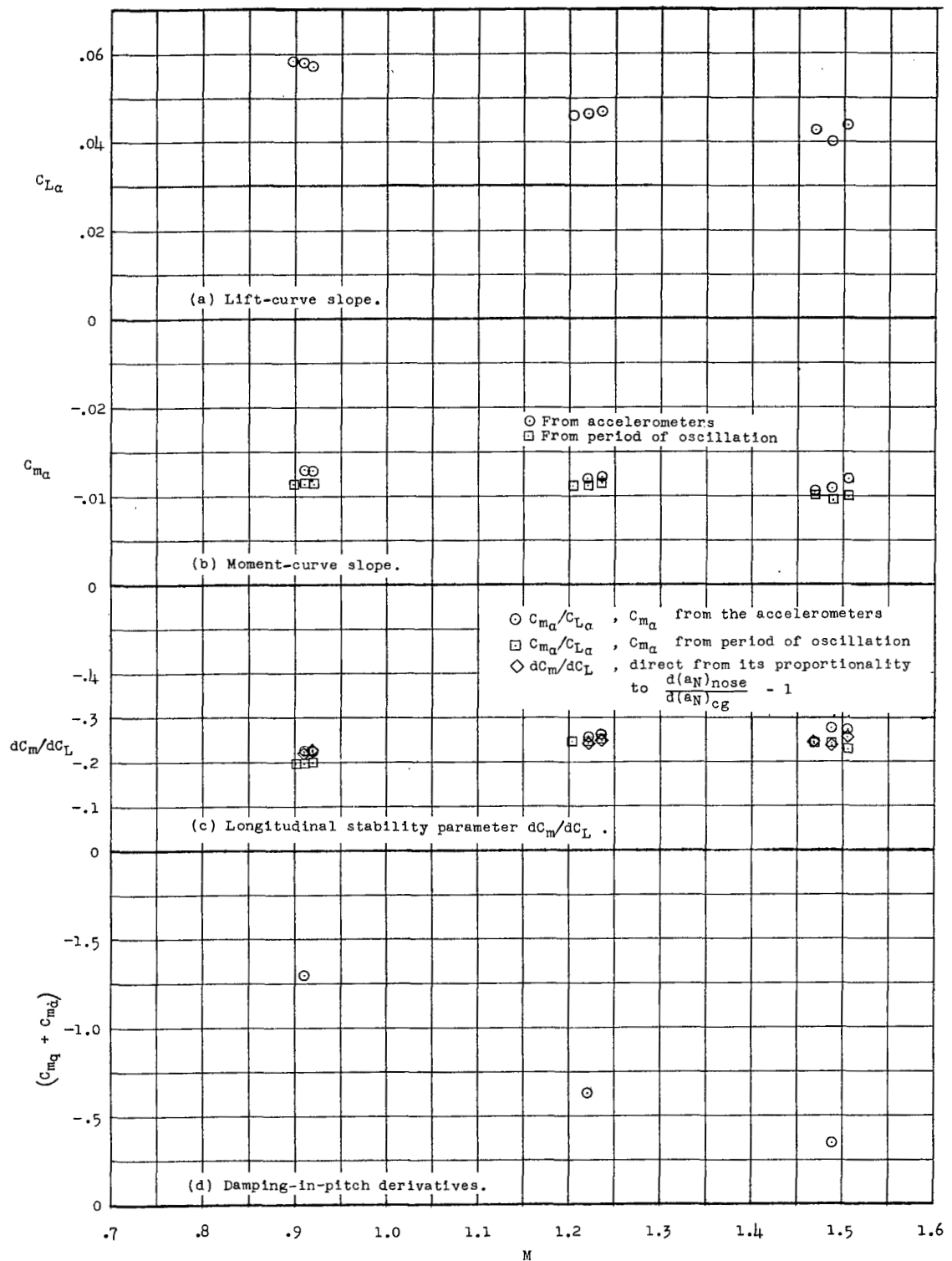
Figure 7.- Longitudinal stability characteristics for model center of gravity at 18.65 percent of the mean aerodynamic chord.
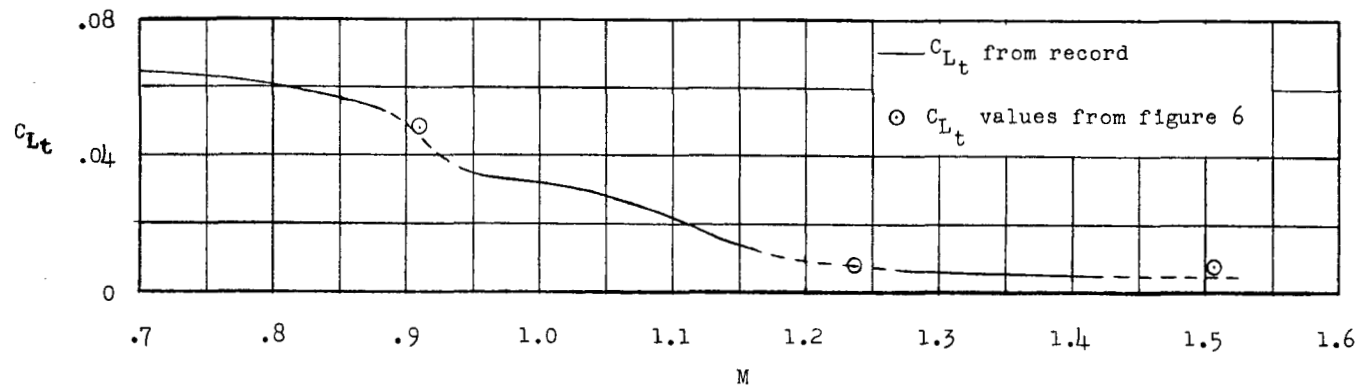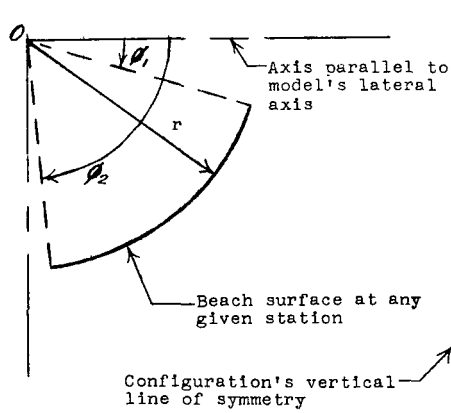
(a) Variation of lift coefficient with Mach number.
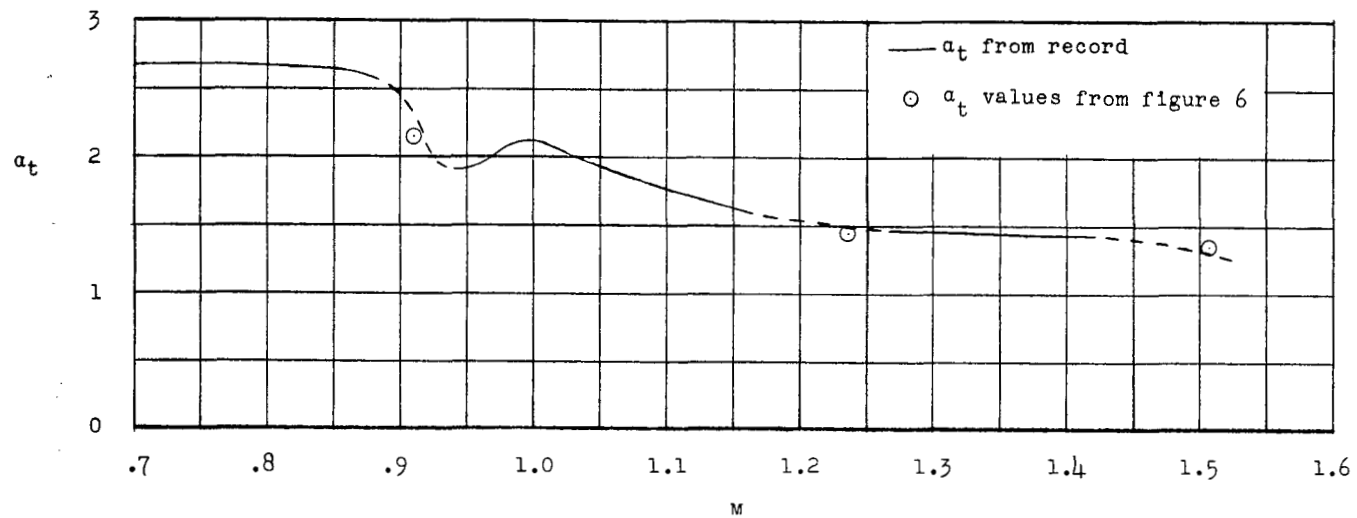
(b) Variation of angle of attack with Mach number.

Figure 8.- Characteristics of the model for trim conditions.
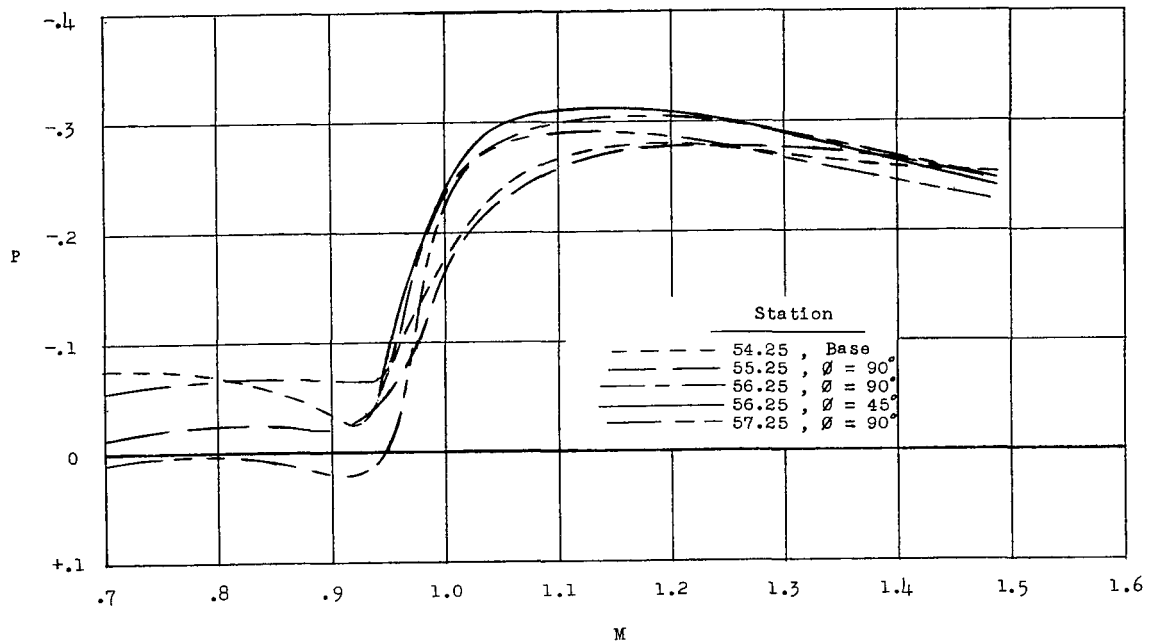
(a) Pressure coefficients.

Station	r	ϕ_1	ϕ_2
54.25	1.38	-90°	+160°
55.25	1.56	-49°	+129°
56.25	1.72	-30°	+115°
57.25	1.90	-16°	+105°
58.00	2.04	- 4°	+ 76°
60.00	2.39	+17°	+ 45°
62.00	2.75	+33°	+ 38°

(b) Sketch and table defining the beach surface.

Figure 9.- Variations of beach pressure coefficients with Mach number. Also shown are a sketch and table by which the beach surface is defined.
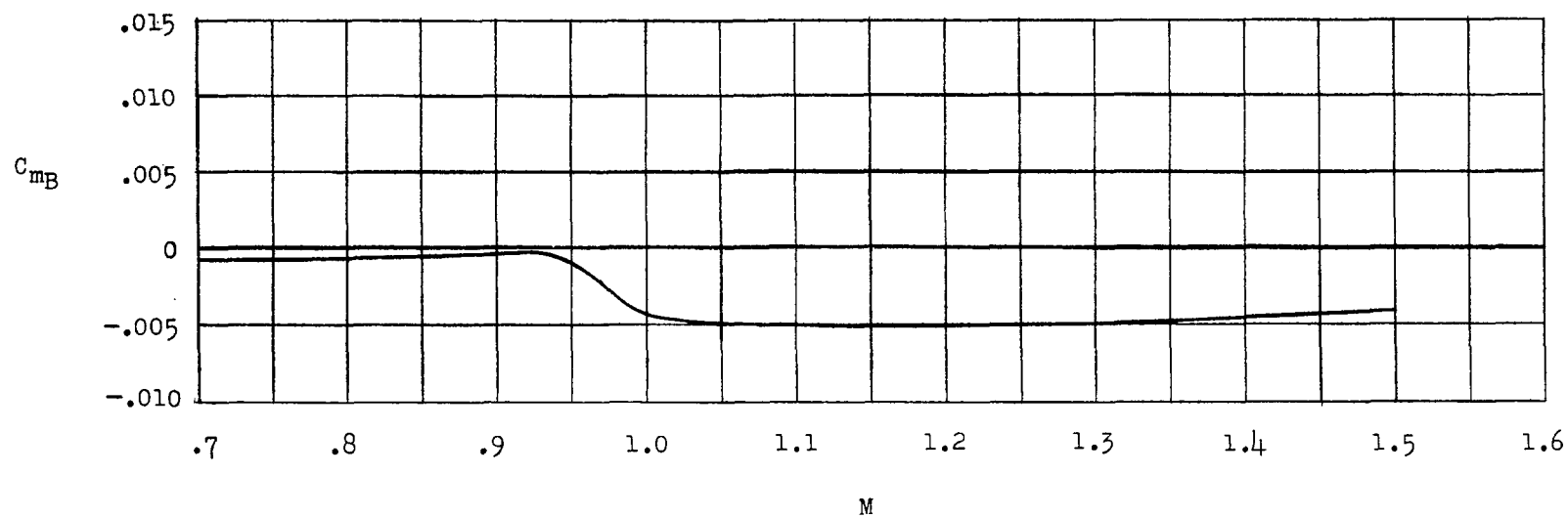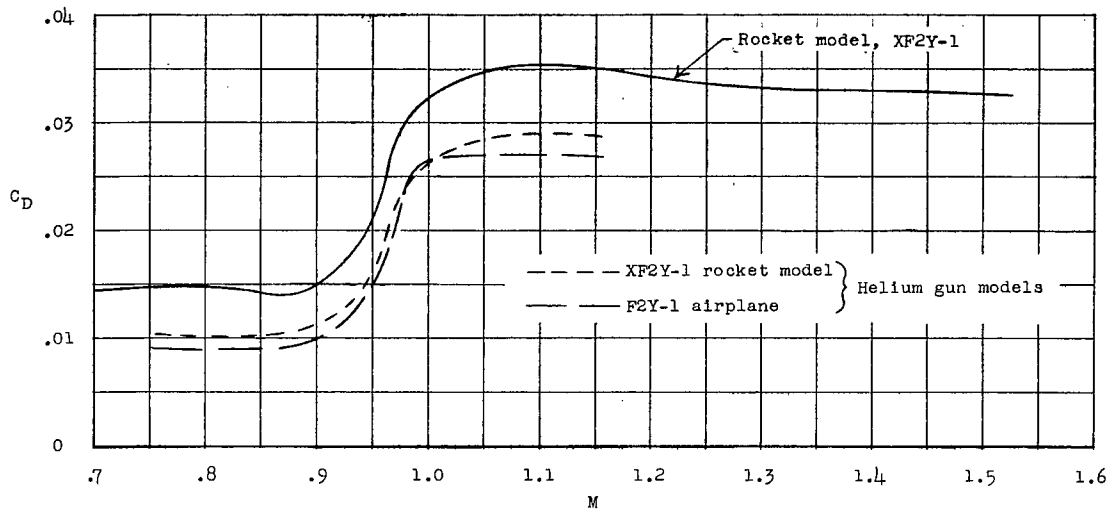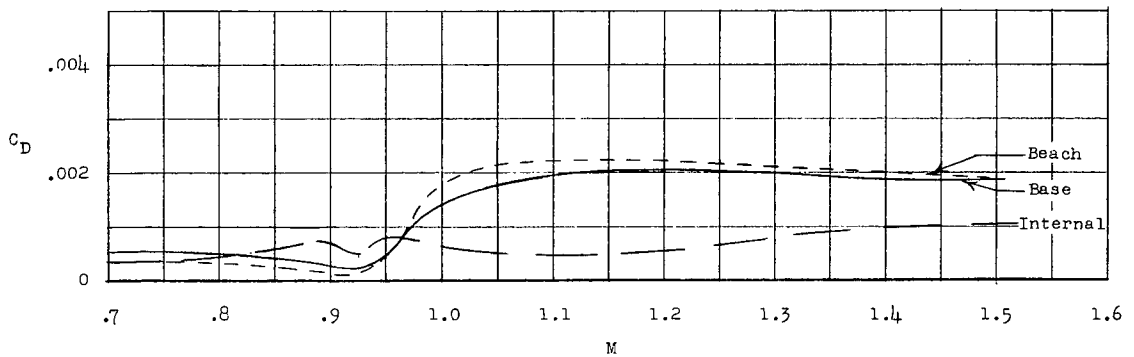
Figure 10.- Pitching-moment coefficient contributed by the beach of the model.

(a) Total configuration drag coefficient.

(b) Component drag coefficient.

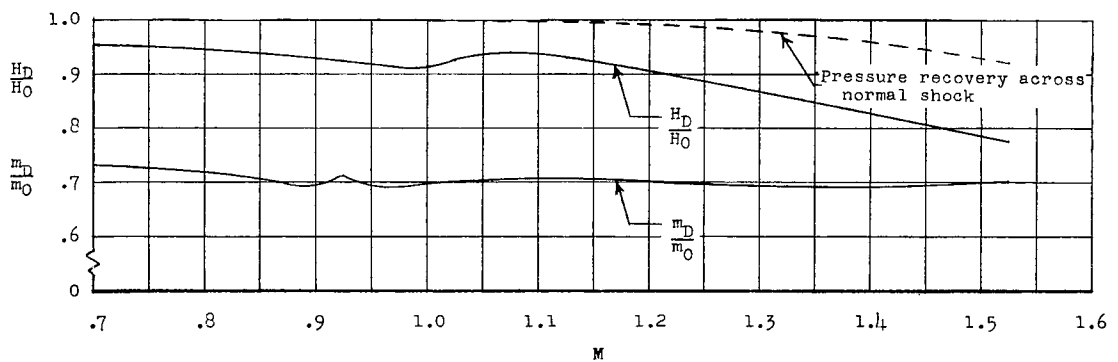Figure 11.- Variation of drag coefficient with Mach number.

Figure 12.- Rocket-model duct characteristics.